



Latitudinal distribution of galactic cosmic ray density and its effect on the CIR-driven modulations of density and density gradient measured by the Muon detector network

Y. OKAZAKI¹, K. MUNAKATA², H. FUKUNISHI¹, A. FUKUSHITA², T. NARUMI², T. CHIBA², S. YASUE³, C. KATO², T. KUWABARA⁴, J. W. BIEBER⁴, P. EVELSON⁴, M. L. DULDIG⁵, J. E. HUMBLE⁶, N. J. SHUCH⁷, M. R. SILVA⁸, A. D. LAGO⁸, I. SABBAH⁹

¹Department of Geophysics, Tohoku University, Japan

²Faculty of Science, Shinshu University, Japan

³School of General Education, Shinshu University, Japan

⁴Bartol Research Institute, University of Delaware, USA

⁵Australian Government Antarctic Division, Australia

⁶School of Mathematics and Physics, University of Tasmania, Australia

⁷Southern Regional Space Research Center, Brazil

⁸National Institute for Space Research, Brazil

⁹Faculty of Science, Kuwait University, Kuwait

okazaki@pat.geophys.tohoku.ac.jp

Abstract: We investigated the unidirectional fractional density gradient in GSE-z (G_{zU}) of Galactic Cosmic Ray (GCR) by using the data obtained by the Muon detector network. The analysis period is from 1994 to 2005. We found that the yearly averaged G_{zU} show temporal variations. It was also found that there is a correlation between the North-South asymmetries of GCR density and solar wind speed at high latitudes. These results suggest that there are some physical connections between them.

Introduction

North-South (NS) asymmetry of Galactic Cosmic Ray (GCR) density with an energy > 100 MeV was observed by the Ulysses spacecraft [1]. The minimum of the latitudinal distribution of GCR density was shifted to the southern hemisphere with $\sim 10^\circ$. Although the initial investigations about solar wind speed and magnetic field did not show the corresponding asymmetries [2, 3], there are some explanations to account for the asymmetry of GCR density. One possible explanation is southward displacement of Heliospheric Current Sheet (HCS) with respect to the solar equatorial plane [4]. Another is overwinding of the Parker spiral field in the southern hemisphere [3]. By using the Neutron detector data (~ 10 GeV), a difference of GCR latitudinal gradients obtained separately in toward and away sectors of the interplanetary magnetic field for the period from 1953 to 1988 was shown [5]. They proposed the

difference would be the unidirectional density gradient caused by NS asymmetry in the solar modulation. However, a decisive mechanism of solar modulation is unresolved although the unidirectional density gradient is correlated with the spiral angle (only during negative solar polarity epoch) and NS asymmetry of sunspot number. The unidirectional latitudinal gradient obtained by the Muon detector network (~ 60 GeV) indicated a higher density of GCR in the southern hemisphere during the Ulysses observation period [6]. This shows an opposite sense in the latitudinal distribution of GCR density measured by the Ulysses. Although this may suggest that the large-scale distribution of high energy GCR is different from that of low energy, the cause also remains unresolved.

In order to reveal the mechanism generating the NS asymmetry of GCR density, we investigated the unidirectional fractional density gradient of GCR in GSE-z to reveal the cause for the NS

asymmetry of GCR density obtained by the Muon detector network. The analysis period is from 1994 to 2005. To examine the displacement of HCS, we obtain the radial solar magnetic field strength (Br) at Earth's orbit in away and toward sectors following [4] and compare it with the unidirectional fractional density gradient of GCR in GSE-z. We also investigate latitudinal distribution of solar wind speed measured by the Interplanetary Scintillation method. We report these results.

Muon detector network

We use the data recorded by two multi-directional Muon detectors at Nagoya (Japan), Hobart (Australia) from 1994 to 1999. And we use the data recorded by three detectors at Nagoya, Hobart and Sao Martinho (Brazil) from 2001 to 2005. For detail properties of the detectors are referenced in [7, 8]. To begin with, we obtain the anisotropy of GCR in the solar wind frame (ξ^w) from the pressure-corrected count rates. The methodology is referenced in [9]. Following [10], we assume the anisotropy perpendicular to the solar wind magnetic field (\mathbf{B}) is predominantly due to $\mathbf{B} \times \nabla n$ drift flux driven by a gradient of GCR density (n). Based on this assumption, the fractional density gradient is given by

$$\mathbf{g}_\perp(t) = R_L \frac{\nabla_\perp n}{n} = -\mathbf{b}(t) \times \xi^w(t) \quad (1)$$

where R_L is the effective particle Larmor radius and $\mathbf{b}(t)$ is a unit vector in the direction of \mathbf{B} .

We average the hourly fractional density gradient data in GSE-z over one Carrington rotation when the longitudinal directions of the solar wind magnetic field are $135 \pm 90^\circ$ (away) and $315 \pm 90^\circ$ (toward), respectively. Hourly solar wind magnetic field data at [11] are used. Moreover, we average these rotational averaged data yearly. 13 or 14 rotational averaged data are used for yearly averages except for 1994 and 1998. Because of a loss of observations, 8 and 10 rotations are used in 1994 and 1998, respectively. Hereafter, the yearly averaged fractional density gradient when the magnetic field directed away from (toward) the Sun is denoted by G_{zA} (G_{zT}). Finally, we sum the G_{zA} and G_{zT} to obtain the unidirectional fractional density gradient (G_{zU}). The value of G_{zU} indicates NS asymmetry of GCR density. For example, if G_{zU} is positive (negative) the GCR density in the

northern hemisphere is higher (lower) than that in the southern hemisphere.

Solar wind magnetic field data

To examine the effect of displacement of HCS [4], we obtain yearly averaged Br in away and toward sectors by using the same procedures as described above. Hourly solar wind magnetic field data at [11] are used. We also obtain yearly averaged observation times in two sectors to deduce displacement of HCS. Yearly averaged Sun's north and south polar fields [12] are also used.

Solar wind speed data

We also investigate latitudinal distributions of solar wind speed. We use the synoptic solar wind speed map deduced by the Interplanetary Scintillation (IPS) measurements carried out by Nagoya University, Japan. Details are referenced in [13]. Fig. 1 shows variations of latitudinal distribution of solar wind speed. Time resolution is one Carrington rotation. The data are missing during winter season for snow coverage. We average the latitudinal distribution of solar wind speed in northern and southern hemispheres over high ($>30^\circ$) and low ($<30^\circ$) latitudes. Finally, these data are averaged yearly. The data which include a loss in the latitudinal distribution are excluded from the yearly average. 6 or 7 rotation data are used for yearly averages. It is noted that the yearly averaged solar wind speed is different from the actual yearly average because available rotations do not cover an entire year. The yearly averaged data in 1994 and 1999 have low reliability since only two rotation data are available.

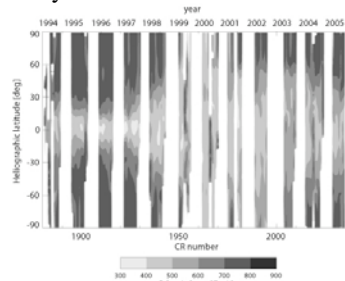


Figure 1: Variations of latitudinal distribution of solar wind speed obtained by the Interplanetary Scintillation (IPS) measurements for the period from 1994 to 2005.

Results and Discussion

Fig. 2a shows variations of G_{zA} , G_{zT} , and G_{zU} from 1994 to 2005. The data for 2000 are excluded because the polarity of the solar magnetic field (\mathbf{A}) is mixed. Before discussing variations of G_{zU} , we refer to the bi-directional fractional density gradient G_{zA} and G_{zT} . The periods from 1994 to 1999 and from 2001 to 2005 correspond to $\mathbf{A}>0$ and $\mathbf{A}<0$ epoch, respectively. It can be found from Fig. 2a that G_{zA} (G_{zT}) is always positive (negative) regardless of \mathbf{A} . This is consistent with the previous studies in different periods [14-16]. These relationships indicate that the latitudinal distribution of GCR density has minimum (maximum) at HCS when $\mathbf{A}>0$ ($\mathbf{A}<0$). This qualitatively supports the calculated latitudinal distribution of GCR density in two polarities [17].

We discuss variations of G_{zU} . An important point from Fig. 2a is that G_{zU} are not time invariant and show temporal variations. For example, whereas the G_{zU} from 1994 to 1999 were nearly zero (NS symmetrical GCR density), the G_{zU} has $\sim 0.1\%$ positive offset (higher density in the northern hemisphere) in 2002 and gradually decreases. In-situ observations made by the Ulysses from Sep. 1994 to Aug. 1995 indicate the existence of a northward (positive) G_{zU} [1]. In our results G_{zU} in 1994 and 1995 are nearly zero. As pointed out by [16], this may suggest a difference of large scale distribution of GCR density between high (~ 60 GeV) and low energies (>100 MeV). It should be noted that we do not consider the NS anti-symmetric component [6] and our results cannot be directly compared with their result. We first investigate the effect of displacement of HCS as proposed by [4]. Figs. 2b and 2c show yearly averaged observation times and Br in two sectors. These two variations show an almost anti-correlation and are considered to indicate displacement of HCS. If Br in the southern hemisphere is greater than that in the northern hemisphere when $\mathbf{A}>0$, southward displacement of HCS would occur. Similarly, if observation time in the away sector is shorter when $\mathbf{A}>0$, southward displacement would occur. Although we can find some NS asymmetries in them, it is difficult to relate these variations to G_{zU} . It can be also said that there are no constant correlation between G_{zU} and the polar field strengths in Fig. 2d. We suggest that the NS asymmetry of GCR density

measured by the Muon detector network is not associated with the displacement of HCS.

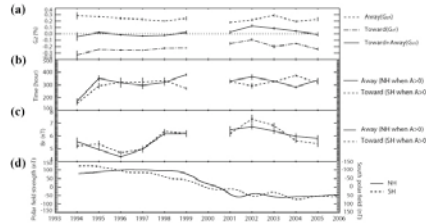


Figure 2: **(a)** Variations of G_{zU} (solid), G_{zA} (dashed) and G_{zT} (dotted-dashed) from 1994 to 2005. The away (toward) sector when $\mathbf{A}>0$ corresponds to the northern (southern) hemisphere. Vertical lines in (a), (b) and (c) show $\pm 1\sigma$ calculated by standard variation of rotational averages in each yearly bin. **(b)** Variations of observation times in away (solid) and toward (dashed) sectors. **(c)** Variations of Br in away (solid) and toward (dashed) sectors. **(d)** Polar field strengths in north (solid) and south (dashed) hemispheres. Sign of the south polar field is inverted.

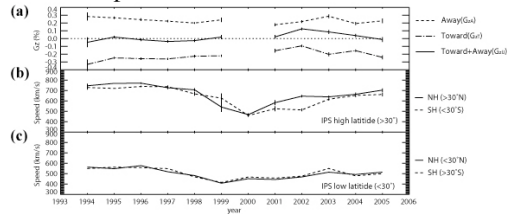


Figure 3: **(a)** Variations of G_{zU} (solid), G_{zA} (dashed) and G_{zT} (dotted-dashed) from 1994 to 2005. (same as Figure 2a). **(b)** Average solar wind speed in northern (solid) and southern (dashed) hemispheres at high latitudes ($>30^\circ$). **(c)** Average solar wind speed in northern (solid) and southern (dashed) hemispheres at low latitudes ($<30^\circ$).

We investigate latitudinal distribution of solar wind speed. It is found from Fig. 3c that there are no NS differences in solar wind speed at low latitudes. On the other hand, we can find NS differences of solar wind speed at high latitudes as shown in Fig. 3b and their correlation with G_{zU} . Nearly zero offset was observed when the latitudinal distribution of solar wind speed is symmetric (1994-1998). In 2002 when the $\sim 0.1\%$ positive offset of G_{zU} was observed, the averaged solar wind speed in the southern hemisphere with $<30^\circ$ was 150 km/s slower than that in the northern hemisphere.

To reveal the physical connection between these two asymmetries, we examine the radial density distribution on the basis of the force-field approximation expressed by

$$\frac{dU}{dr} = \frac{UCV_{sw}}{K} \quad (2)$$

where U is the GCR density, V_{sw} is the solar wind speed, K is the diffusion coefficient and C is the Compton-Getting factor. Using the observation values in 2002, we deduce the radial diffusion coefficient (K_{rr}) using the theoretical Parker spiral angle (ψ). The equation is expressed by

$$\tan \psi = \frac{2\pi r \sin \theta}{V_{sw} T}, \quad (3)$$

where θ is the heliographic latitude, r is the radius, and T is the Sun's rotation period. Taking $\theta = \pm 45^\circ$, $r=1$ AU, $T=27$ days, V_{sw} at latitude of $45^\circ = 650$ km/s (northern), 500 km/s (southern), we obtain $\psi = 24^\circ, 30^\circ$. The equation of K_{rr} is expressed by

$$K_{rr} = K_{\parallel} \cdot \cos^2 \psi + K_{\perp} \cdot \sin^2 \psi \quad (4)$$

where K_{\parallel} and K_{\perp} are the diffusion coefficient parallel and perpendicular to the magnetic field. Taking $K_{\perp} = 0.05 K_{\parallel}$ and $\psi = 24^\circ, 30^\circ$, K_{rr} is $\sim 10\%$ smaller in the southern hemisphere at latitudes of 45° than that in the northern hemisphere. This leads to a decrease of GCR density in the southern hemisphere. However, the solar wind speed in the southern hemisphere is $\sim 30\%$ slower than in the northern hemisphere. That is, the sum of the effects of NS asymmetries of the K_{rr} and the solar wind speed would cause an increase of GCR density in the southern hemisphere. This shows an opposite sense to the observation results. We have no clear theory to account for the physical connection between the two asymmetries. It seems to be difficult to explain the cause of the asymmetry using the force-field approximation.,

Summary

The results obtained in this study are summarized as follows.

- Values of G_{zU} from 1994 to 2005 are not time invariant and show temporal variations.
- It is found that the displacement of HCS would not be considered to be the cause for the GCR asymmetry obtained by the Muon detector network.

- Variations of G_{zU} show a correlation with the NS asymmetry of solar wind speed.

These results suggest that there are some physical connections between the NS asymmetries of GCR density and solar wind speed. To explain the connection quantitatively is the future subject.

Acknowledgement

The solar wind magnetic field data are downloaded from the OMNIweb service. We also thank the WSO for providing the polar field data.

References

- [1] Simpson, J. A., Zhang, M., and Bame, S. (1996), *Astrophys. J.*, 465, L69.
- [2] Phillips, J. *et al.* (1995), *Geophys. Res. Lett.*, 22, 3301.
- [3] Forsyth, R. J. *et al.* (1996), *Astron. Astrophys.*, 316, 287.
- [4] Smith, E. J. *et al.* (2000), *Astrophys. J.*, 533, 1084.
- [5] Chen, J., J. W. Bieber and M. A. Pomerantz (1991), *J. Geophys. Res.*, 96, 11569.
- [6] Munakata, K., *et al.* (1999), *Adv. Space. Res.*, 23, 459.
- [7] Munakata, K., *et al.* (2000), *J. Geophys. Res.*, 105, 27,457.
- [8] Munakata, K., *et al.* (2001), Conf. Pap. Int. Cosmic Ray Conf. 27th, 9, 3494.
- [9] Kuwabara, T., *et al.* (2004), *Geophys. Res. Lett.*, 31, L19803.
- [10] Bieber, J. W., and P. Evenson (1998), *Geophys. Res. Lett.*, 25, 2955.
- [11] [<http://omniweb.gsfc.nasa.gov/ow.html>]
- [12] [<http://wso.stanford.edu/Polar.html>]
- [13] Kojima, M. *et al.* (2001), *J. Geophys. Res.*, 106, 15677.
- [14] Bieber, J. W., and J. Chen (1999), *Astrophys. J.*, 372, 301.
- [15] Chen, J., J. W. Bieber (1993), *Astrophys. J.*, 405, 375.
- [16] Munakata, K., *et al.* (2002), *Adv. Space. Res.*, 29, 1523.
- [17] Kota, J. and J. R. Jokipii (1983), *Astrophys. J.*, 265, 573.